Millijoule femtosecond pulses at 1937 nm from a diode-pumped ring cavity Tm:YAP regenerative amplifier

Seyed Ali Rezvani, Makoto Suzuki, Pavel Malevich, Clément Livache, Jean Vincent de Montgolfier, Yutaka Nomura, Noriaki Tsurumachi, Andrius Baltuška, Takao Fuji

Research Article | Vol. 26, No. 22 | 29 Oct 2018 | OPTICS EXPRESS 29460
Optics EXPRESS

Millijoule femtosecond pulses at 1937 nm from a diode-pumped ring cavity Tm:YAP regenerative amplifier

SEYED ALI REZVANI,[1,*] MAKOTO SUZUKI,[2] PAVEL MALEVICH,[3] CLEMENT LIVACHE,[1,4] JEAN VINCENT DE MONTGOLFIER,[1,5] YUTAKA NOMURA,[1] NORIAKI TSURUMACHI,[2] ANDRIUS BALTUŠKA,[3] AND TAKAO FUJI[1]

[1] *Institute for Molecular Science, 38 Nishigonaka, Myodaiji, Okazaki, 444-8585, Japan*
[2] *Faculty of Engineering, Kagawa University, 2217-20 Hayashi-cho, Takamatsu, 761-0396, Japan*
[3] *Photonics Institute, TU Wien, Gusshausstrasse 27-387, Vienna A-1040, Austria*
[4] *Laboratoire de Physique et d'Étude des Matériaux, ESPCI-Paris, PSL Research University, Sorbonne Université Univ Paris 06, CNRS UMR 8213, 10 rue Vauquelin 75005 Paris, France*
[5] *École Nationale Supérieure de Chimie de Paris (Chimie ParisTech), 11 rue Pierre et Marie Curie, Paris, 75005 France*
[*] *rezvani@ims.ac.jp*

Abstract: We present an infrared source operating at 1937 nm center wavelength capable of generating 1.35 mJ pulse energies with 1 kHz repetition rate and 2 GW peak power based on a diode-pumped Tm:YAP regenerative amplifier. The obtained pulses after 45 round trips have been compressed down to 360 fs. Using only a small portion (15 µJ) of the output of the system we managed to generate a white light continuum in a 3 mm YAG window that exhibits the viability of the system as a suitable candidate for a pumping source of a mid-infrared optical parametric amplifier.

1. Introduction

Intense ultrashort infrared (IR) pulses play a pivotal role in many of the current research fields and applications. Powerful femtosecond pulses in the vicinity of 2 µm are highly desired for coherent mid-infrared (MIR) [1–5] or terahertz (THz) pulse generation [6], high harmonic generation reaching soft x-ray in water-window [7–9], and atmospheric sensing [10]. In order to obtain intense femtosecond pulses around the 2 µm wavelength region, one of the most widely used schemes is optical parametric amplification (OPA) with well-established ultrafast pump lasers such as Ti:sapphire or Yb lasers. The OPA provides highly tunable IR pulses and has expanded our reach to the realm of few-cycle pulse duration limits [11–16].

However, OPA in general has complicated design due to the requirements of the precise synchronization between the pump and seed pulses while a very high intensity pump pulse is required for triggering the parametric amplification. This fact attracts a lot of attentions to the development of solid-state lasers, directly generating high energy ultrashort pulses around 2 µm, such as Tm:YAP, Ho:YAG, Ho:YLF, or Cr:ZnSe [17–22]. Regenerative or multi-pass amplifiers based on these materials can scale up nJ pulses directly to mJ energy levels while each material has its own advantages and disadvantages.

Cr:ZnSe has a large emission cross section and broadband gain spectrum. Very recently, sub-100-fs and multi-millijoule pulse generation at 2.5 µm has been demonstrated [22]. However, since its lifetime is only ~6 µs it is necessary to use a high energy nanosecond laser at around 2 µm, for example a thulium fiber laser pumped Q-switched Ho:YAG laser, as a pump source for such lasers. This would make the system highly complex and expensive.

The emission cross section of holmium is in fact higher than of the thulium's, and efficient

#341237 https://doi.org/10.1364/OE.26.029460
Journal © 2018 Received 31 Jul 2018; revised 16 Sep 2018; accepted 19 Sep 2018; published 26 Oct 2018

amplification is possible. The generation of 39 mJ 10 ps pulses at 100 Hz repetition rate has been demonstrated [23]. However, the gain bandwidth is narrower than that of the other materials, and generation of sub-picosecond pulses is still challenging even with the manipulation of the seed spectrum [18, 19] or the gain spectrum in the amplifier [20]. Moreover, the absorption wavelength is ~1.9 µm, where diode lasers are not common. Usually, a high power continuous wave thulium fiber laser is used for pumping the holmium gain media.

On the other hand, femtosecond lasers based on thulium can be pumped by laser diodes operating at 794 nm center wavelength which makes them very attractive as versatile practical systems, although the emission cross section is not as large as that of the holmium's. Such laser diode sources are well developed and easily accessible while they are inexpensive and very compact [24].

Actually, very strong amplification and broadband gain spectrum can be achieved with thulium-doped fibers. Highly developed fiber lasers, capable of generating several hundred micro joules [25, 26] and more than tens of gigawatt peak power, have been achieved using external pulse compression [27]. However, millijoule energy level is still highly challenging for fiber lasers.

Thulium-doped $YAlO_3$ (Tm:YAP) in comparison with the other commercially available candidates in this category like Tm:YAG or Tm:YLF, has a higher emission cross section [10] while its natural birefringence makes the alignment process easier. This makes it suitable as a gain medium of a regenerative amplifier at this wavelength.

In this work we present a new scheme that solely based on Tm:YAP takes the capability of such lasers to 2 GW peak power after compression, using a ring cavity regenerative amplifier design. A supercontinuum has been generated in a 3 mm YAG crystal using a small portion of the system output (15 µJ) which exhibits the viability of the proposed system as a great candidate for MIR-OPA systems as a straightforward pumping source.

2. Experimental setup

The schematic of the experimental setup is depicted in Fig. 1. The seeding source in our scheme is an upgraded version of the double-cladding, clad pumped, Tm:ZBLAN fiber oscillator described in [28], generating 80 fs pulses with 52 MHz repetition rate and 4 nJ energy. These pulses are sent to a Martinez stretcher based on a transmission grating (560 grooves/mm) and a concave mirror (CCM1, r=1500 mm). This provides 16 ps^2 of group delay dispersion (GDD) and the pulse is stretched to ~100 ps. The throughput of the stretcher is ~10%. The stretched pulses are sent to a ZBLAN fiber pre-amplifier consisting of a 2.6 m long double-clad 2% thulium-doped ZBLAN fiber with the core and clad diameter of 20 and 200 µm. The fiber is pumped in a counter-propagation direction by a laser diode centered at 794 nm [29]. The seed pulses are amplified up to ~100 nJ with 11.5 W pump power. The amplified pulses are picked with 1 kHz repetition rate by a Pockels cell and are sent to the regenerative amplifier.

The cavity of the regenerative amplifier is ring and the Pockels cell in the cavity is under $\lambda/2$ operation. We opted for a ring cavity to avoid a Faraday rotator inside the cavity, which may limit the highest pulse energy. The gain medium of the regenerative amplifier is a 12 mm long, c-axis cut Tm:YAP crystal with 4% doping concentration. It is wrapped in indium foil and stationed on a module made of metalized copper and cooled using a thermoelectric unit which can provide low and stable temperature down to −20°C to increase the single pass gain. Because of the re-absorption of the thulium, these crystals are sensitive to the changes in temperature [30]. The crystal is pumped using a multi-mode fiber coupled laser diode with the fiber core diameter of 200 µm and numerical aperture of 0.22 which is capable of generating 31 watts of output power centered at 794 nm. The pump is focused into the crystal using a f=250 mm achromatic lens and passes through a dichroic mirror. In the end, the diameter of the pump beam inside the crystal is 0.5 mm. The absorption in the crystal is around 75% for all applied input powers which for the

Optics EXPRESS

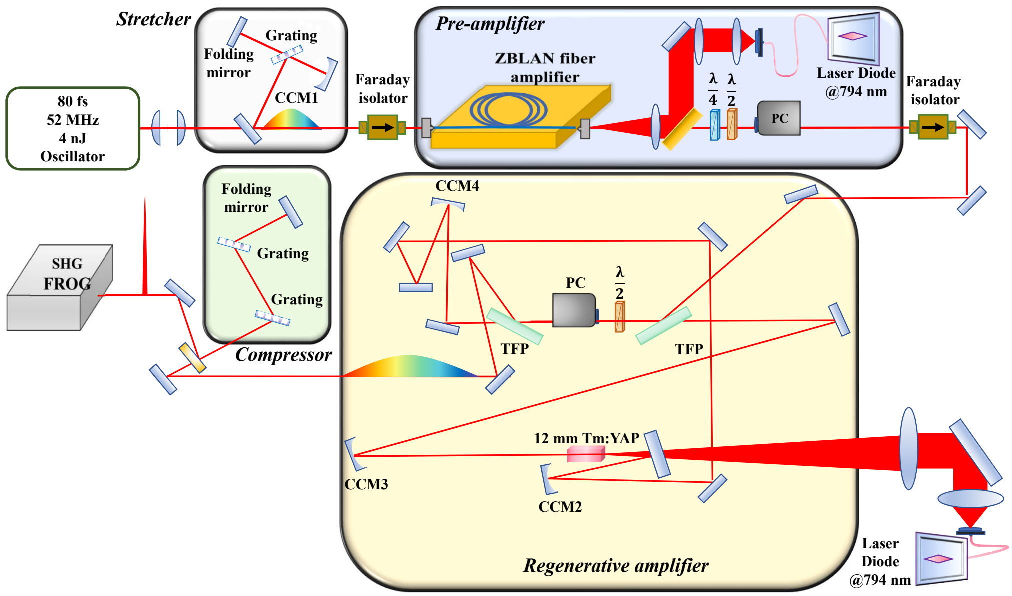

Fig. 1. The schematic design of the system. CCM represents concave mirrors, CCM1 (r=1500 mm), CCM2 and CCM3 (r=500 mm), and CCM4 (r=3000 mm). TFP, thin film polarizer. PC, Pockels cell.

maximum input results in 23.5 W absorbed power in the crystal.

The water absorption for the region of our interest plays a huge role in the obtainable spectrum for the amplified pulses [17, 18], therefore, the amplification stage is usually enclosed in a chamber purged by an inert gas. This part of the system in our scheme is purged with nitrogen to decrease the present humidity to lower than 7% values. Purging the system has resulted in the direct reduction of the effect of the water absorption on the amplified signal spectrum at each round trip that has been observed in the previously published literature [17] and can be recognized through cross referencing with the high-resolution transmission molecular absorption database (HITRAN). The obtained pulses after the amplification are sent to a pair of transmission gratings made of fused silica with 66% efficiency and 560 grooves/mm that are placed at the distance of 57 cm from each other introducing -13.2 ps^2 GDD.

3. Experimental results

The performance of the system has been investigated at two different temperatures, 19°C and −20°C. The system has been purged with nitrogen when the temperature is −20°C. Figure 2 illustrates the changes of the obtained output of the system for the two different temperatures. Using similar conditions at 19°C we can only obtain the slope efficiency of 8.1% which is much less than of the value obtained for the low temperature case. As it can be seen from the Fig. 2, the amplification is triggered at different absorbed power values but similarly for both cases, the output linearly scales up with the pumping power at these values. The slope efficiency of the system exhibits an obvious increase operating at −20° (23.2%) compared to the slope efficiency at 19°C. The maximum output of the system running at 1 kHz and 45 round trips at −20°C reaches 1.35 mJ using 23.5 W absorbed power. For this case the B-integral value is estimated to be 5.12.

The amplified pulses are centered at 1937 nm, the spectrum of the signal is depicted in Fig. 3. The effect of the water absorption on the spectrum has been considerably reduced by purging the system, but the spectrum shows features that are resulted from traveling in the 7% humidity.

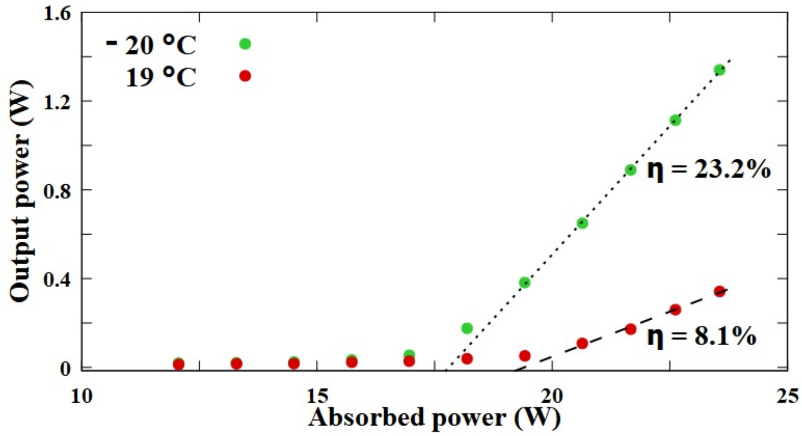

Fig. 2. Corresponding output power of the system to the absorbed power for 19°C and air (red circles), −20°C and purged with nitrogen (green circles).

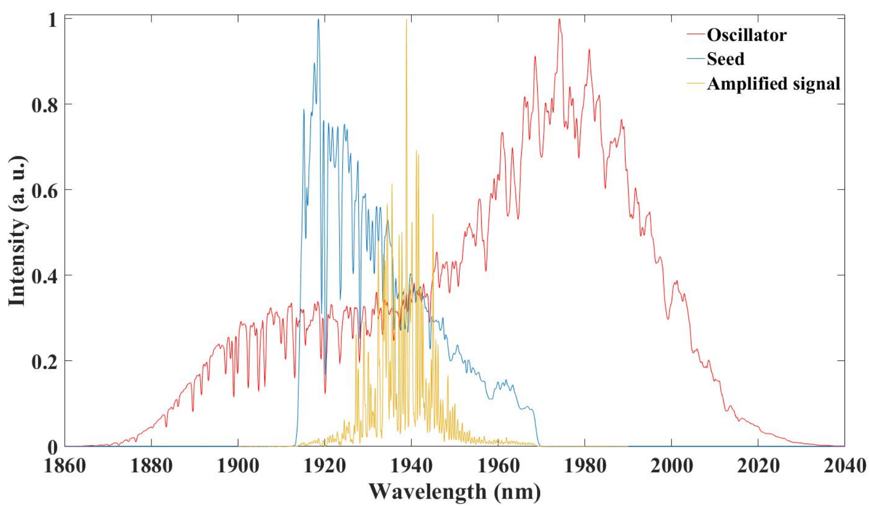

Fig. 3. Spectrum of the amplified signal with 1.35 mJ energy with 23.5 W absorbed power at −20°C and 1 kHz repetition rate, recorded by using an optical spectrum analyzer (Yokogawa AQ6375) with the resolution of 0.02 nm. The blue line represents the spectrum of the seed after the fiber amplifier.

We actually installed a vacuum chamber for the cavity and evacuated the air in the cavity down to ~0.01 mbar to minimize the effect of the water vapor, however, the spectrum did not change dramatically. We have studied the effect of the water absorption in our system through changing the number of round trips. The spectrum of the system pumped with 23.5 W absorbed power, is recorded for three different values of 36, 45 and 64 round trips and the results are presented in Fig. 4. Even though higher number of round trips results in higher obtainable output energies, however, the lengthening of the optical path causes the effect of water absorption to accumulate and the spectrum modulation to increase, as seen on the recorded spectra. For the case of 64 round trips, we observe the loss of spectral components, and the pulse eventually exhibits much narrower bandwidth. Here, we have chosen 45 round trips as a good trade off between the

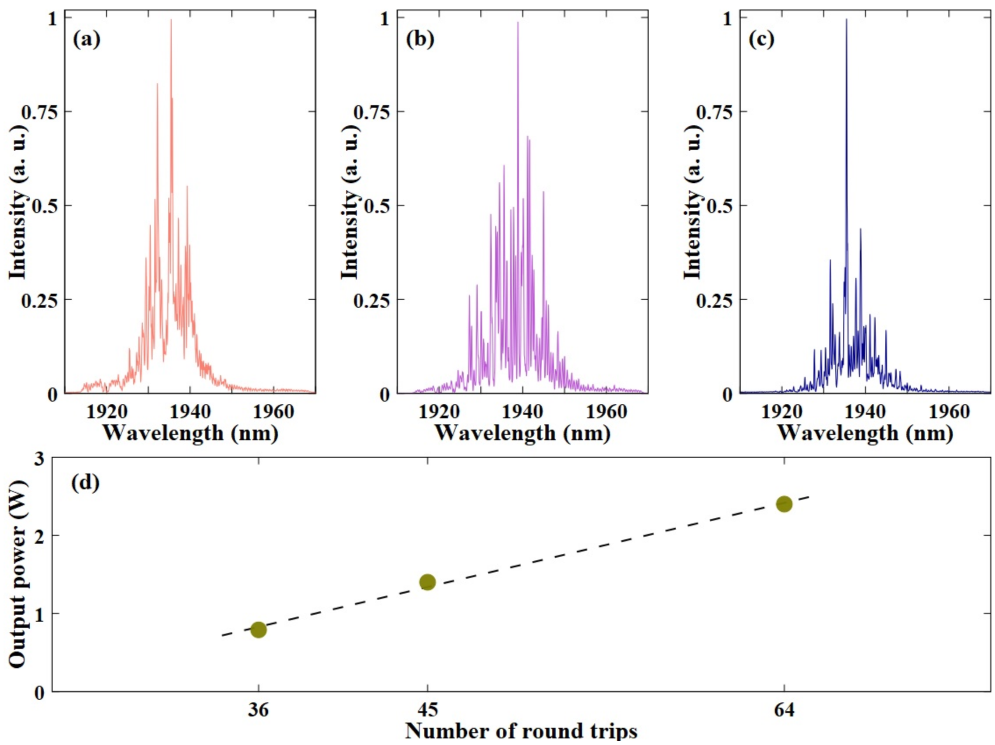

Fig. 4. Spectrum of the amplified beam with the resolution of 0.02 nm at −20° after (a) 36 , (b) 45 and (c) 64 round trips. (d) The evolution of the system output power with the increase in the round trip.

obtainable energy and spectral bandwidth.

The temporal profile of the system in the case of 45 round trips has been investigated after the compression using a home-built second-harmonic generation frequency resolved optical gating system (SHG-FROG) [31] and the results are depicted in Fig. 5. In order to characterize the pulse with such a complex structured spectrum, we need to scan the delay in a long range (∼ ±40 ps) and resolve the spectrum with a high resolution (∼0.2 nm). We have measured a lot of satellite signals, which come from the fine structure of the spectrum, in the several tens of picosecond range in the FROG trace. The intensity of the largest satellite is below 10% of the intensity of the main pulse. As can be seen in Fig. 5(b), all the satellites are well-retrieved. As a result, the overall feature of the spectrum is well-retrieved with a reasonable FROG error (∼0.2%). We have actually found out that the largest satellite at 22.5 ps delay actually comes from the reflection of the back surface of the thin film polarizer (corresponding to traveling time, propagating through 2×3.3 mm of fused silica) in the cavity. The duration of the main part of the pulse is estimated as 360 fs, corresponding to 2 GW peak power. The intensities of the satellites are so small that the peak intensity of the main part is preserved well (80% of the pulse energy is maintained under the main pulse).

The capabilities of the system has been further investigated for the application in high intensity regimes, where it might be necessary, and the output of the system has been recorded for the 500 Hz repetition rates at −20°C. For the maximum absorbed power of 23.5 W, pulses with 2.4 mJ output energy have been observed (B-integral of 8.58). The obtainable output power and spectrum of the system for this configuration are depicted in Fig. 6, the dotted line on the Fig. 6(a) depicts the slope efficiency of the system (η=13.15%). The spectrum is basically the same as the

Optics EXPRESS

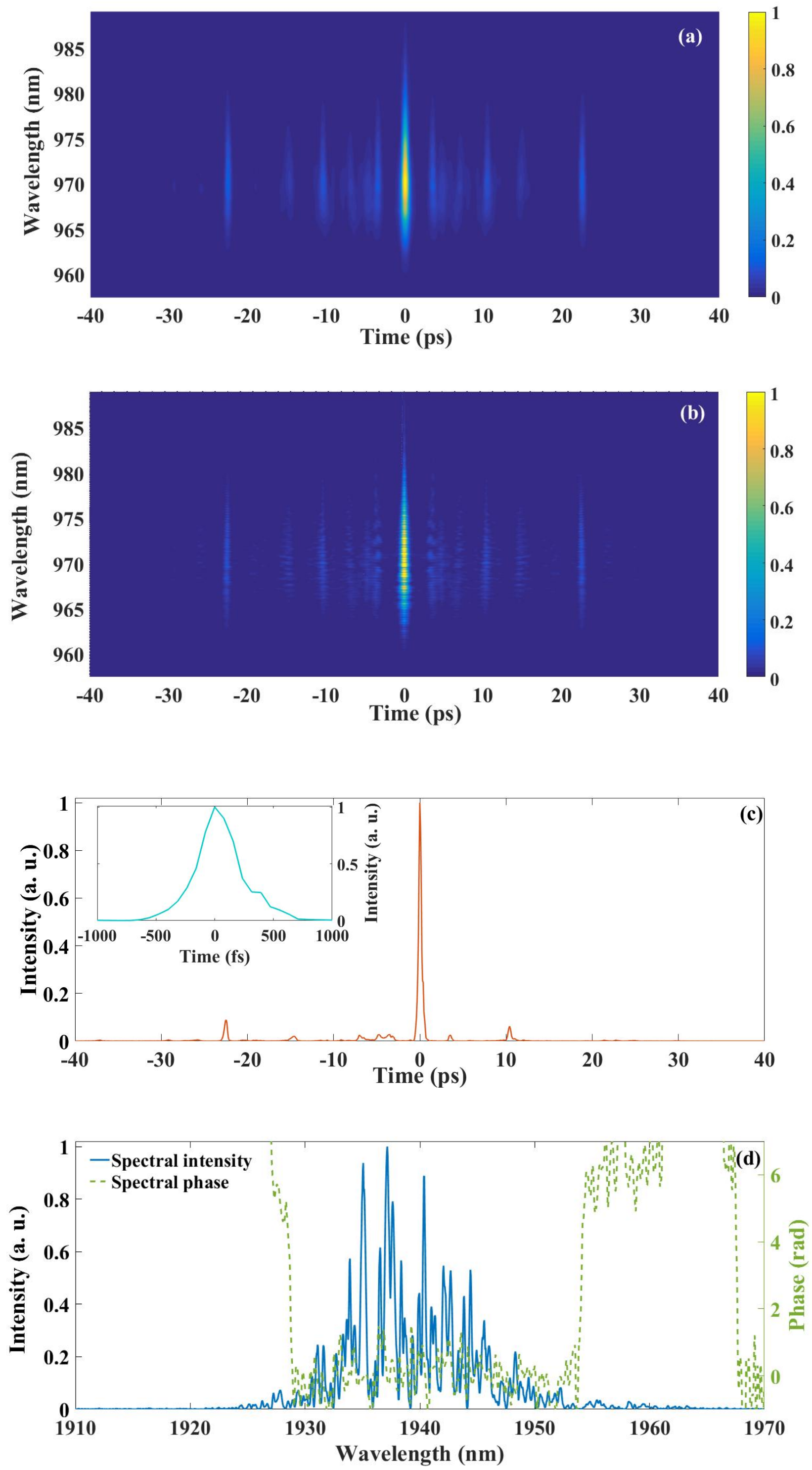

Fig. 5. (a) Measured FROG trace,(b) retrieved FROG trace with 0.002 best error value in a 2048×2048 grid, (c) retrieved temporal profile, inset: zoomed view of the main pulse peak, (d) retrieved power spectrum and spectral phase.

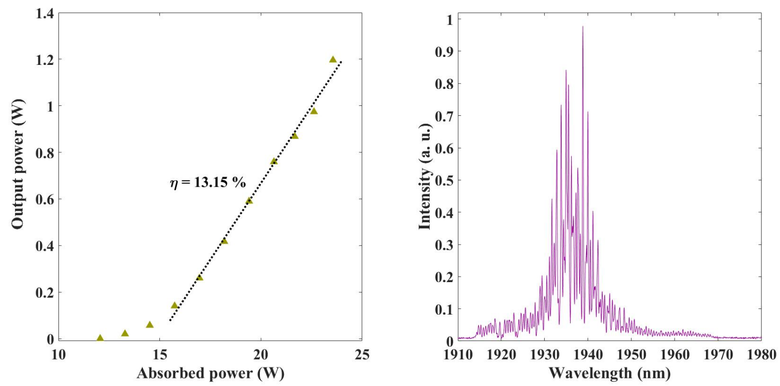

Fig. 6. (a) Obtained output power corresponding to the absorbed power, (b) recorded spectrum with the resolution of 0.02 nm.

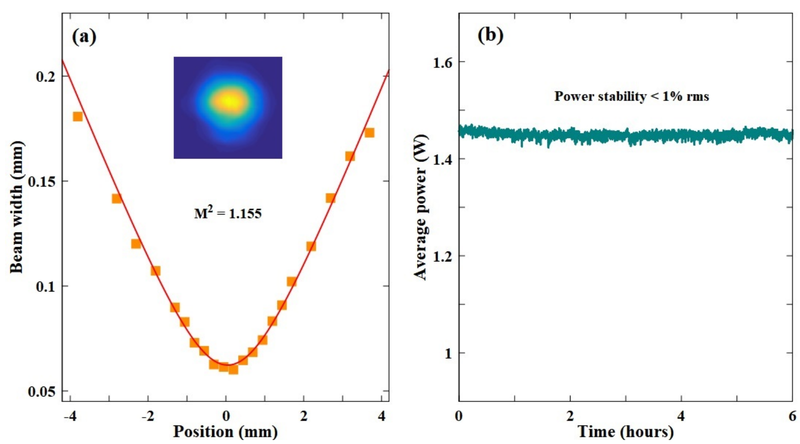

Fig. 7. (a) M^2 measurement results. Inset: beam profile recorded after compression and before entering the lens. (b) Long-term power stability of the system over the period of 6 hours.

1 kHz repetition rate case, which means that no serious nonlinear effect exists in the laser system at this energy level. Bifurcation effect can occur at repetition rates close to the inverse of the upper state lifetime [21, 32–35]. It is not observed here for neither 500 Hz nor 1 kHz. However, this effect was seen when generating millijoule pulses without the fiber preamplifier, that is when the gain of the main amplifier is very high.

The beam quality of the system after the compression has been investigated focusing it with a f=100 mm lens and recording the beam width by a pyroelectric camera (Ophir Pyrocam IV) in combination with an imaging optics. The beam profiles have been recorded for a series of points by moving the camera in the focal direction. The beam width for each point is obtained by calculating the $D4\sigma$. Using the measured values the M^2 can be obtained for the beam. The obtained pulses after compression have shown a good profile (M^2=1.15) which is depicted in Fig. 7(a). In fact, the beam diameter varies for the threshold pump powers to the maximum power due to the thermal lensing effect. An increase of 21% has been observed on the beam diameter from 4.2 mm at the threshold pump power to 5.1 mm at the maximum pump power. Another important property for a light source, specially one which can be used for applications such as

Optics EXPRESS

HHG and OPA is its stability. We have recorded the output of the system over a period of 6 hours and the system has exhibited a long-term power stability of less than 1% RMS. The results are presented in Fig. 7(b).

4. White light generation

The proposed system has exhibited capability of generating gigawatt peak intensities in a straightforward and simple design which makes it a good candidate for application in OPA systems as a powerful pumping source.

In order to illustrate our setup's viability for the application in such systems we have generated white light in a bulk medium which is the basis of many of the OPA schemes. YAG crystals have been shown to be suitable bulk media for white light generation using infrared sources [36–40]. We have used a 3 mm YAG window for this purpose. Using only a small portion of the compressed signal (15 μJ) we have managed to successfully generate white light in the crystal. The spectrum of the generated white light is presented in Fig. 8. The spectrum seems to extend outside the measurement range, however, we did not have a spectrometer supporting outside the range. Nevertheless, it is clear that the generated white light can be used as the seed for MIR-OPA applications, at least idler waves >8.6 μm can be generated with the spectral component between 2.0–2.5 μm. The changes of the generated white light with the pump intensity has been investigated by changing the position of the YAG crystal relative to the focal point and the results for three different positions are also depicted in Fig. 8. As expected, the extents of the generated spectrum increases with the increase in the pump intensity.

The availability of the 2 μm femtosecond pulses to trigger such nonlinear interactions in bulk material plays a pivotal role in the quality and simplicity of the broadband OPA operating in MIR range. The phase quality of the femtosecond white light seed source is usually so high that the spectral phase can be controlled. In the case of the OPA based on picosecond lasers the seed source could be derived from optical parametric generation (OPG), which is a stochastic process that starts from vacuum noise and therefore its phase is based on vacuum noise and cannot be controlled, in particular, the carrier-envelope phase [41]. OPG sources suffer from inherently large shot-to-shot energy fluctuations which when used as a seed would result in an unstable source and poor spatial beam quality [42]. Otherwise the picosecond pump lasers are optically or

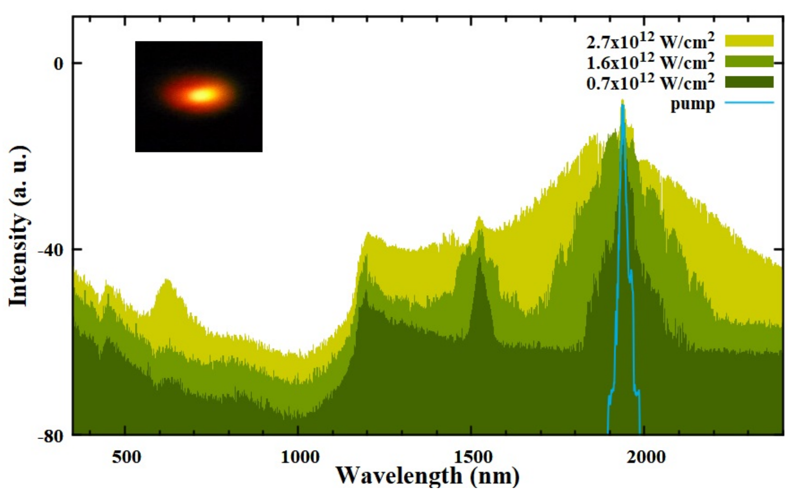

Fig. 8. Variation of the generated white light with the changes of the pump intensity. Inset: a photograph of the white light.

electronically synchronized with a femtosecond laser which is capable of producing broadband seed for the OPA [3]. However, the synchronization of the pump and seed pulses of the OPA becomes much more complex than femtosecond laser based OPA.

Generation of femtosecond white light seeding source also provides the possibility of having variety of OPA designs. We can design a kHz repetition rate OPA, which is suitable for spectroscopic applications, by using the femtosecond pulse as the pump and white light as the seed. On the other hand, we can design a high pulse energy OPA, which is suitable for strong field applications, through using a DC-OPA scheme [43], namely, using the uncompressed pulse as the pump pulse and the compressed pulse as the white light generator.

5. Conclusion

The proposed scheme, in a ring cavity regenerative amplifier design solely based on Tm:YAP and pumped by laser diodes, generates millijoule level femtosecond pulses centered at 1937 nm with 2 GW peak power at 1 kHz repetition rate. Pulses were successfully compressed with a pair of transmission gratings and the retrieved SHG-FROG trace reveals 360 fs pulses duration. The emission bandwidth of the gain medium of the regenerative amplifier is actually much broader than the bandwidth of the final output of the amplifier. The gain narrowing effect can be compensated by using some spectral filtering for the seed and/or inside the cavity of the amplifier. Furthermore, external pulse compression using a hollow core fiber [44] or multi-plate compression [45] would provide an ideal light source for HHG.

The compressed pulses exhibit good beam profile and can be directly used to generate white light in bulk materials. Such properties combined with the good power scalability over a wide range of available pumping energies and the perfect stability over long running periods of time makes this scheme a viable candidate for either direct application in MIR-OPA systems or a pumping source for a spectrally broadened pumped OPA systems [14]. In particular, the system exhibits a flexible electronic control on the obtainable output energy through changes in round trips, pumping energy, and repetition rate which make it a good candidate for many applications such as spectroscopy which would require a tight control over the light source. The proposed ring regenerative amplifier provides a versatile and simple IR source that can be used in many of the current applications, in a compact table-top design.

Funding

SENTAN (JST, Japan Science and Technology); Consortium for Photon Science and Technology (JST); the Joint Studies Program (2016-2018) of the Institute for Molecular Science; Core Research for Evolutional Science and Technology (CREST) (JPMJCR17N5).

Acknowledgments

The authors acknowledge Masatoshi Nishio and Sakae Kawato of Fukui University for significant contribution to the initial stage of the thulium regenerative amplifier development. The authors would like to thank Yoshinori Mimura and Kazuhiko Ogawa of FiberLabs Inc., who provided the ZBLAN fibers used for the oscillator and fiber amplifier. In addition, they gave us many insightful comments and suggestions.

References

1. N. Leindecker, A. Marandi, R. L. Byer, K. L. Vodopyanov, J. Jiang, I. Hartl, M. Fermann, and P. G. Schunemann, "Octave-spanning ultrafast OPO with 2.6-6.1 µm instantaneous bandwidth pumped by femtosecond Tm-fiber laser," Opt. Express **20**, 7046–7053 (2012).
2. H. Liang, Z. W. Peter Krogen, H. Park, T. Kroh, K. Zawilski, P. Schunemann, J. Moses, L. F. DiMauro, F. X. Kärtner, and K. H. Hong, "High-energy mid-infrared sub-cycle pulse synthesis from a parametric amplifier," Nat. Commun. **8**, 141 (2017).

3. D. Sanchez, M. Hemmer, M. Baudisch, S. L. Cousin, K. Zawilski, P. Schunemann, O. Chalus, C. Simon-Boisson, and J. Biegert, "7 μm, ultrafast, sub-millijoule-level mid-infrared optical parametric chirped pulse amplifier pumped at 2 μm," Optica **3**, 147–150 (2016).
4. T. Kanai, P. Malevich, S. S. Kangaparambil, K. Ishida, M. Mizui, K. Yamanouchi, H. Hoogland, R. Holzwarth, A. Pugzlys, and A. Baltuška, "Parametric amplification of 100 fs mid-infrared pulses in $ZnGeP_2$ driven by a Ho:YAG chirped-pulse amplifier," Opt. Lett. **42**, 683–686 (2017).
5. P. Malevich, T. Kanai, H. Hoogland, R. Holzwarth, A. Baltuška, and A. Pugžlys, "Broadband mid-infrared pulses from potassium titanyl arsenate/zinc germanium phosphate optical parametric amplifier pumped by Tm, Ho-fiber-seeded Ho:YAG chirped-pulse amplifier," Opt. Lett. **41**, 930–933 (2016).
6. M. Clerici, M. Peccianti, B. E. Schmidt, L. Caspani, M. Shalaby, M. Giguère, A. Lotti, A. Couairon, F. Légaré, T. Ozaki, D. Faccio, and R. Morandotti, "Wavelength scaling of terahertz generation by gas ionization," Phys. Rev. Lett. **110**, 253901 (2013).
7. H. Xiong, H. Xu, Y. Fu, J. Yao, B. Zeng, W. Chu, Y. Cheng, Z. Xu, E. J. Takahashi, K. Midorikawa, X. Liu, and J. Chen, "Generation of a coherent x ray in the water window region at 1 kHz repetition rate using a mid-infrared pump source," Opt. Lett. **34**, 1747–1749 (2009).
8. N. Ishii, S. Adachi, Y. Nomura, A. Kosuge, Y. Kobayashi, T. Kanai, J. Itatani, and S. Watanabe, "Generation of soft x-ray and water window harmonics using a few-cycle, phase-locked, optical parametric chirped-pulse amplifier," Opt. Lett. **37**, 97–99 (2012).
9. K. H. Hong, C. J. Lai, J. P. Siqueira, P. Krogen, J. Moses, C.-L. Chang, G. J. Stein, L. E. Zapata, and F. X. Kärtner, "Multi-mJ, kHz, 2.1 μm optical parametric chirped-pulse amplifier and high-flux soft x-ray high-harmonic generation," Opt. Lett. **39**, 3145–3148 (2014).
10. K. Scholle, S. Lamrini, P. Koopmann, and P. Fuhrberg, "2 μm laser sources and their possible applications," in "Frontiers in Guided Wave Optics and Optoelectronics," , B. Pal, ed. (IntechOpen, Rijeka, 2010), chap. 21.
11. N. Ishii, K. Kaneshima, K. Kitano, T. Kanai, S. Watanabe, and J. Itatani, "Sub-two-cycle, carrier-envelope phase-stable, intense optical pulses at 1.6 μm from a BiB_3O_6 optical parametric chirped-pulse amplifier," Opt. Lett. **37**, 4182–4184 (2012).
12. J. Darginavičius, N. Garejev, and A. Dubietis, "Generation of carrier-envelope phase-stable two optical-cycle pulses at 2 μm from a noncollinear beta-barium borate optical parametric amplifier," Opt. Lett. **37**, 4805–4807 (2012).
13. Y. Deng, A. Schwarz, H. Fattahi, M. Ueffing, X. Gu, M. Ossiander, T. Metzger, V. Pervak, H. Ishizuki, T. Taira,
T. Kobayashi, G. Marcus, F. Krausz, R. Kienberger, and N. Karpowicz, "Carrier-envelope-phase-stable, 1.2 mJ, 1.5 cycle laser pulses at 2.1 μm," Opt. Lett. **37**, 4973–4975 (2012).
14. S. A. Rezvani, Z. Hong, X. Pang, S. Wu, Q. Zhang, and P. Lu, "Ultrabroadband tunable OPA design using a spectrally broadened pump source," Opt. Lett. **42**, 3367–3370 (2017).
15. Y. Yin, J. Li, X. Ren, K. Zhao, Y. Wu, E. Cunningham, and Z. Chang, "High-efficiency optical parametric chirped-pulse amplifier in BiB_3O_6 for generation of 3 mJ, two-cycle, carrier-envelope-phase-stable pulses at 1.7 μm," Opt. Lett. **41**, 1142–1145 (2016).
16. Z. Hong, S. A. Rezvani, Q. Zhang, W. Cao, and P. Lu, "Ultrabroadband microjoule 1.8 μm laser pulse from a single-stage broadband pumped OPA," Opt. Lett. **43**, 3706–3709 (2018).
17. A. Wienke, D. Wandt, U. Morgner, J. Neumann, and D. Kracht, "700 MW peak power of a 380 fs regenerative amplifier with Tm:YAP," Opt. Express **23**, 16884–16889 (2015).
18. A. Wienke, D. Wandt, U. Morgner, J. Neumann, and D. Kracht, "Comparison between Tm:YAP and Ho:YAG ultrashort pulse regenerative amplification," Opt. Express **24**, 8632–8640 (2016).
19. P. Malevich, G. Andriukaitis, T. Flöry, A. J. Verhoef, A. Fernández, S. Ališauskas, A. Pugžlys, A. Baltuška, L. H. Tan, C. F. Chua, and P. B. Phua, "High energy and average power femtosecond laser for driving mid-infrared optical parametric amplifiers," Opt. Lett. **38**, 2746–2749 (2013).
20. K. Murari, H. Cankaya, P. Kroetz, G. Cirmi, P. Li, A. Ruehl, I. Hartl, and F. X. Kärtner, "Intracavity gain shaping in millijoule-level, high gain Ho:YLF regenerative amplifiers," Opt. Lett. **41**, 1114–1117 (2016).
21. L. von Grafenstein, M. Bock, D. Ueberschaer, U. Griebner, and T. Elsaesser, "Ho:YLF chirped pulse amplification at kilohertz repetition rates - 4.3 ps pulses at 2 μm with GW peak power," Opt. Lett. **41**, 4668–4671 (2016).
22. X. Ren, L. H. Mach, Y. Yin, Y. Wang, and Z. Chang, "Generation of 1 kHz, 2.3 mJ, 88 fs, 2.5 μm pulses from a Cr^{2+}:ZnSe chirped pulse amplifier," Opt. Lett. **43**, 3381–3384 (2018).
23. M. Hemmer, D. Sánchez, M. Jelínek, V. Smirnov, H. Jelinkova, V. Kubeček, and J. Biegert, "2-μm wavelength, high-energy Ho:YLF chirped-pulse amplifier for mid-infrared OPCPA," Opt. Lett. **40**, 451–454 (2015).
24. H. Q. Le, W. D. Goodhue, P. A. Maki, and S. D. Cecca, "Diode-laser-pumped InGaAs/GaAs/AlGaAs heterostructure lasers with low internal loss and 4-W average power," Appl. Phys. Lett. **63**, 1465–1467 (1993).
25. F. Stutzki, C. Gaida, M. Gebhardt, F. Jansen, C. Jauregui, J. Limpert, and A. Tünnermann, "Tm-based fiber-laser system with more than 200 MW peak power," Opt. Lett. **40**, 9–12 (2015).
26. C. Gaida, M. Gebhardt, F. Stutzki, C. Jauregui, J. Limpert, and A. Tünnermann, "Thulium-doped fiber chirped-pulse amplification system with 2 GW of peak power," Opt. Lett. **41**, 4130–4133 (2016).
27. M. Gebhardt, C. Gaida, F. Stutzki, S. Hädrich, C. Jauregui, J. Limpert, and A. Tünnermann, "Nonlinear pulse compression to 43 W GW-class few-cycle pulses at 2 μm wavelength," Opt. Lett. **42**, 747–750 (2017).
28. Y. Nomura, M. Nishio, S. Kawato, and T. Fuji, "Development of ultrafast laser oscillators based on thulium-doped ZBLAN fibers," IEEE J. Sel. Top. Quantum Electron. **21**, 0900107 (2015).

Optics EXPRESS

29. Y. Nomura and T. Fuji, "Efficient chirped-pulse amplification based on thulium-doped ZBLAN fibers," Appl. Phys. Express **10**, 012703 (2017).
30. S. A. Payne, L. L. Chase, L. K. Smith, W. L. Kway, and W. F. Krupke, "Infrared cross-section measurements for crystals doped with Er^{3+}, Tm^{3+}, and Ho^{3+}," IEEE J. Quantum Electron. **28**, 2619–2630 (1992).
31. K. W. DeLong, R. Trebino, J. Hunter, and W. E. White, "Frequency-resolved optical gating with the use of second-harmonic generation," J. Opt. Soc. Am. B **11**, 2206–2215 (1994).
32. P. Kroetz, A. Ruehl, G. Chatterjee, A.-L. Calendron, K. Murari, H. Cankaya, P. Li, F. X. Kärtner, I. Hartl, and R. J. D. Miller, "Overcoming bifurcation instability in high-repetition-rate Ho:YLF regenerative amplifiers," Opt. Lett. **40**, 5427–5430 (2015).
33. L. von Grafenstein, M. Bock, G. Steinmeyer, U. Griebner, and T. Elsaesser, "Taming chaos: 16 mJ picosecond Ho:YLF regenerative amplifier with 0.7kHz repetition rate," Laser Photon. Rev. **10**, 123–130 (2016).
34. L. von Grafenstein, M. Bock, U. Griebner, and T. Elsaesser, "High-energy multi-kilohertz Ho-doped regenerative amplifiers around 2 µm," Opt. Express **23**, 14744–14752 (2015).
35. L. von Grafenstein, M. Bock, D. Ueberschaer, U. Griebner, and T. Elsaesser, "Picosecond 34 mJ pulses at kHz repetition rates from a Ho:YLF amplifier at 2 μm wavelength," Opt. Express **23**, 33142–33149 (2015).
36. A.-L. Calendron, H. Çankaya, G. Cirmi, and F. X. Kärtner, "White-light generation with sub-ps pulses," Opt. Express **23**, 13866–13879 (2015).
37. F. Silva, D. R. Austin, A. Thai, M. Baudisch, M. Hemmer, D. Faccio, A. Couairon, and J. Biegert, "Multi-octave supercontinuum generation from mid-infrared filamentation in a bulk crystal," Nat. Commun. **3**, 807 (2012).
38. A. Dubietis, G. Tamošauskas, R. Šuminas, V. Jukna, and A. Couairon, "Ultrafast supercontinuum generation in bulk condensed media," Lith J. Phys. **57**, 113–157 (2017).
39. I. Gražulevičiūtė, M. Skeivytė, E. Keblytė, J. Galinis, G. Tamošauskas, and A. Dubietis, "Supercontinuum generation in YAG and sapphire with picosecond laser pulses," Lith J. Phys. **55**, 110–116 (2015).
40. N. Garejev, G. Tamošauskas, and A. Dubietis, "Comparative study of multioctave supercontinuum generation in fused silica, YAG, and LiF in the range of anomalous group velocity dispersion," J. Opt. Soc. Am. B **34**, 88–94 (2017).
41. C. Manzoni, G. Cirmi, D. Brida, S. De Silvestri, and G. Cerullo, "Optical-parametric-generation process driven by femtosecond pulses: Timing and carrier-envelope phase properties," Phys. Rev. A **79**, 033818 (2009).
42. C. Manzoni and G. Cerullo, "Design criteria for ultrafast optical parametric amplifiers," J. Opt. **18**, 103501 (2016).
43. Q. Zhang, E. J. Takahashi, O. D. Mücke, P. Lu, and K. Midorikawa, "Dual-chirped optical parametric amplification for generating few hundred mJ infrared pulses," Opt. Express **19**, 7190–7212 (2011).
44. M. Nisoli, S. De Silvestri, and O. Svelto, "Generation of high energy 10 fs pulses by a new pulse compression technique," Appl. Phys. Lett. **68**, 2793–2795 (1996).
45. C.-H. Lu, Y.-J. Tsou, H.-Y. Chen, B.-H. Chen, Y.-C. Cheng, S.-D. Yang, M.-C. Chen, C.-C. Hsu, and A. H. Kung, "Generation of intense supercontinuum in condensed media," Optica **1**, 400–406 (2014).